ELSEVIER

Journal of Molecular Catalysis A: Chemical 98 (1995) 15–24

JOURNAL OF MOLECULAR CATALYSIS A: CHEMICAL

A theoretical study of Ziegler–Natta olefin polymerization on the $TiCl_3$ crystalline surface

Akinobu Shiga [a,*], Hiroshi Kawamura-Kuribayashi [b], Toshio Sasaki [b]

[a] *Tsukuba Research Laboratory, Sumitomo Chemical Co., Ltd., 6 Kitahara, Tsukuba 300-32, Japan*

[b] *Chiba Research Laboratory, Sumitomo Chemical Co., Ltd., 2-1, Kitasode, Sodegaura-shi, Chiba 299-02, Japan*

Received 19 April 1994; accepted 4 November 1994

Abstract

Olefin insertion into Ti–methyl bonds of methyltitanium chloride clusters on a $TiCl_3$ crystalline surface has been studied by using paired interacting orbitals (PIO). We have shown that at least two types of active sites can be assumed on the edge of the basal face of violet $TiCl_3$ crystallites: a edge type active site which possesses a dangling bonded Cl atom, four bridged Cl atoms and a Cl vacancy and a corner type active site which possesses a dangling bonded Cl atom, three bridged Cl atoms and two Cl vacancies. The size effects on these active site have been estimated by changing the number of titanium atoms of the $TiCl_3$ model clusters. The most important interaction in the olefin coordinated state is electron delocalization from the occupied Ti d_{xz} orbital of the methyltitanium chlorides to the π^* orbital of the coordinated olefin molecule, while in the transition state is electron delocalization from the occupied C p and Ti d_{xz} orbital of the methyltitanium chloride species to the π^* orbital of the olefin. These interactions are compactly shown in PIO's. The coordination energy and the activation energy for the olefin insertion are almost independent of the cluster size when the number of Ti atoms is greater than three. The corner type active site has been shown to be stabilized at the transition state by the absence of one of the Cl atoms which are located orthogonal to the insertion plane. Thus, the olefin insertion on the corner type active site is more favorable than that on the edge type active site. In the case of propylene insertion, *syn*-orientation of propylene is favored. This regioselectivity should be lower on the corner type active site than that on the edge type active site.

1. Introduction

One of the most important discoveries in this century in chemistry and in chemical industries is the Ziegler–Natta catalysts for polymerization of olefins. The highly active heterogeneous catalysts have modernized the polyolefins manufacturing processes and now gas phase processes are becoming the main stream of new production technologies. As the manufacturing processes become more efficient, more sophisticated catalysts which are able to control molecular weight and its distribution, copolymerization ratio, regio- and stereo-selectivities and so on, are also required to give polymers with desirable chemical and physical properties. Since the discovery of highly active homogeneous metallocene catalysts by Kaminsky et al. [1], much interest has been directed to homogeneous catalysts, because of their possibilities of producing versatile polymers: syndiotactic polypropylene, syndiotactic polystyrene, ethylene/α-olefin copolymer with very narrow MWD etc. It is important to know the factors that play crucial roles in the polymerization proc-

* Corresponding author.

SSDI 1381-1169(95)00002-X

esses in order to develop new sophisticated catalysts.

A number of studies have been reported on the mechanism of polymerization by heterogeneous Ziegler–Natta catalysts [2]. Though the Cossee mechanism has widely been accepted as the most plausible [3], it is still qualitative. Novaro et al. [4] first studied the ethylene insertion process in the Cossee mechanism by means of ab initio restricted Hartree–Fock calculations. They verified the concerted motion that had been proposed by Armstrong et al. [5], and estimated the activation energy roughly to be 15 kcal mol^{-1}. Recent developments in ab initio molecular orbital computational methods make it possible to determine the potential-energy profile of a full catalytic cycle [6]. Kawamura et al. [7] have reported the potential-energy profile of the olefin insertion which is the essential step in the Cossee polymerization mechanism. Jolly and Marynick [8] reported the direct insertion polymerization of ethylene by a real Ziegler–Natta initiator system, $[Cp_2TiCH_3]^+$. The activation energy obtained was 9.8 kcal mol^{-1} using ab initio calculations with MP2-level corrections.

From a practical point of view, ab initio calculations are not easy to apply to the large catalytic systems used in industry. In addition, molecular orbitals spread over the whole molecular system and, therefore, it is not easy to understand the interactions between two large molecules.

Fujimoto et al. [9] proposed a method of determining unequivocally the orbitals which should play dominant roles in interactions between two systems. Then, interactions were represented compactly in terms of a few pairs of localized orbitals. In each orbital pair, one orbital belongs to one fragment species and the other orbital to the other fragment species. They called those orbitals 'paired interacting orbitals' (PIO). Although this analysis was proposed originally for ab initio calculations, we reported that this approach was also useful in analyzing the results of extended Hückel calculations [10]. This method is particularly of use as a conventional tool to gain insight into the role of complicated catalytic systems, such as industrial Ziegler–Natta catalysts, without invoking time-consuming calculations.

In this paper we study olefin polymerization on a $TiCl_3$ crystalline surface with a view to obtaining information useful for development of new homogeneous so-called single site catalysts. This study consists of three parts.

1: modeling of an active site; we cut off titanium chloride clusters $[Ti_nCl_m]^{-m+3n}$ from the edge and the corner of the basal face of α-$TiCl_3$ crystallite as a precursor of the active site.

2: orbital interactions in ethylene insertion of the methyl–Ti bond of the active site; we analyze the π complex and the transition state by using PIO.

3: factors affecting the insertion process; we discuss effects of the size of the cluster and the geometry of propylene insertion.

2. Method

2.1. Elucidation of an active site model

Many kinetic, morphological and crystallographic studies of heterogeneous polymerization catalysts have revealed that the violet $TiCl_3$ catalyst is composed of agglomerates of microcrystallites and the precursor of an active site is located on the edge of the basal face of violet $TiCl_3$ crystalline surfaces. It has a Cl vacancy and a dangling boned Cl atom with a dangling bond which is alkylated by an alkylaluminum co-catalyst to form the active site [2]. The formation of an active site is illustrated schematically in Fig. 1.

Fig. 2 shows the structure of a $CH_3Ti_{16}Cl_{47}$ cluster which has been removed from the edge of the basal face of the violet $TiCl_3$ crystalline. One sees that at least two types of active sites are formed, one on the edge and the other on the corner of the crystalline. The former is an [Oh-CH_3TiCl_4], having one Cl vacancy, and the latter is an [Oh-CH_3TiCl_3], having two Cl vacancies. The central titanium atoms of them are Ti: 1 and Ti: 4 shown in Fig. 2, respectively.

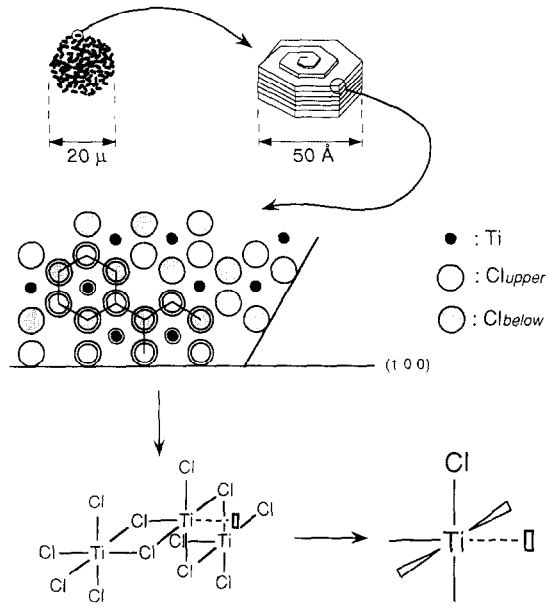

Fig. 1. A sketch of the active site on the $TiCl_3$ crystalline surface.

We examine several numbers of $[CH_3Ti_nCl_m$ $(n=1–5)]$ clusters for the edge type active site and $[CH_3Ti_4Cl_{13}]$ cluster for the corner type active site in order to clarify the effect of size and geometry of the clusters. They are shown in Fig. 3.

2.2. PIO analysis

We have examined an olefin coordinated state and a transition state based on the Cossee insertion mechanism as shown Fig. 4. The geometry optimization technique was not adopted for determining the structures of these states. We assumed their structures on the basis of those reported previously [9]. The details of these models are given in the Appendix. We then divided a model complex (combined system C) into a methyltitanium chloride portion (fragment A) and an olefin molecule (fragment B) as shown in Fig. 5. The geometries of [A] and [B] were the same as those in the original complex ([A–B] ≡ [C]).

The molecular orbitals of [A], [B] and [C] were calculated by the extended Hückel method [11]. The extended Hückel parameters are given in the Appendix. PIOs were obtained by applying the procedure that was proposed by Fujimoto et al. [4]. It is summarized as follows:

1. we expand the MOs of a complex in terms of the MOs of two fragment species, to determine the expansion coefficients $c_{i,f}$, $c_{m+j,f}$ and $d_{k,f}$, $d_{n+l,f}$ in Eq. 1

$$\Phi_f = \sum_{i=1}^{m} C_{i,f}\phi + \sum_{j=1}^{M-m} C_{m+j,f}\phi_{m+j} + \sum_{k=1}^{n} d_{k,f}\psi_k + \sum_{l=1}^{N-n} d_{n+l,f}\psi_{n+1}$$

$$f = 1, 2, \ldots, m+n \qquad (1)$$

where Φ, is a MO of the complex [C], ϕ and ψ are the MOs of the fragment [A] and [B] respectively, m and n indicate the number of the occupied MOs of A and of B, respectively, and M and N represent the number of the MOs of A and of B, respectively.

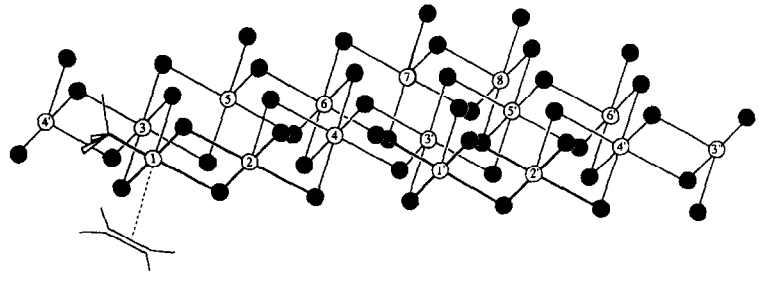

Olefin insertion into Ti-methylbond

on the $TiCl_3$ crystalline surface

Fig. 2. $CH_3Ti_{16}Cl_{47}$ cluster cut off from the edge of the lateral face of α-$TiCl_3$.

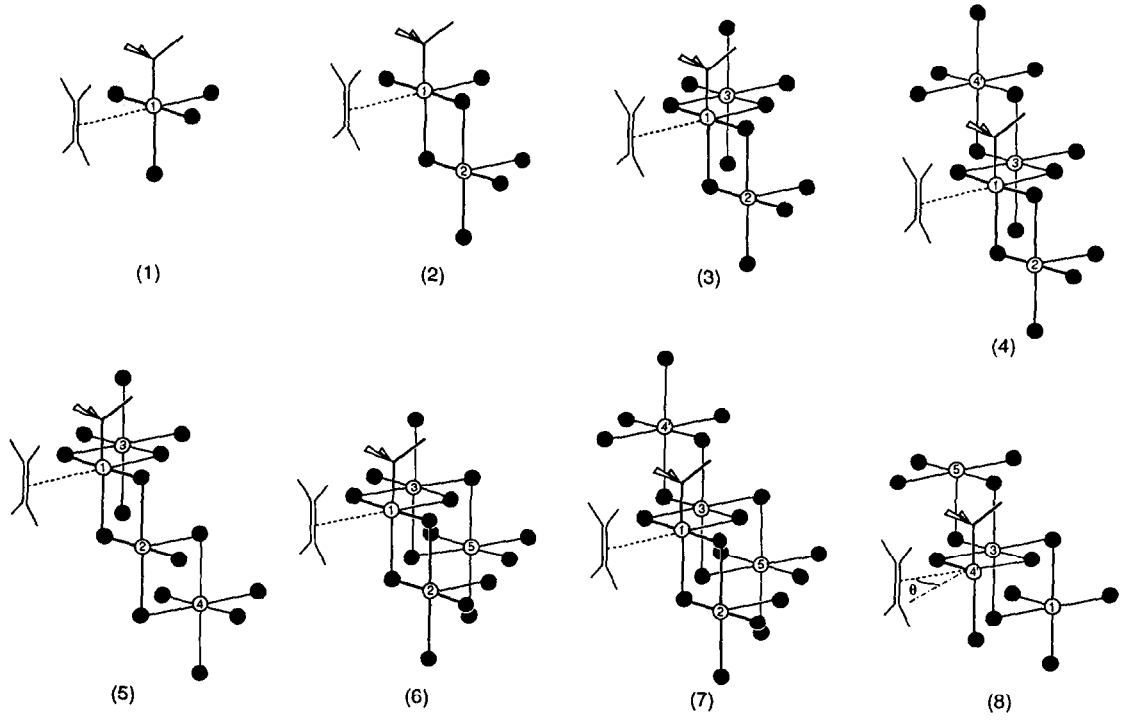

Fig. 3. [$CH_3Ti_nCl_m$ (n: 1–5)] model clusters.

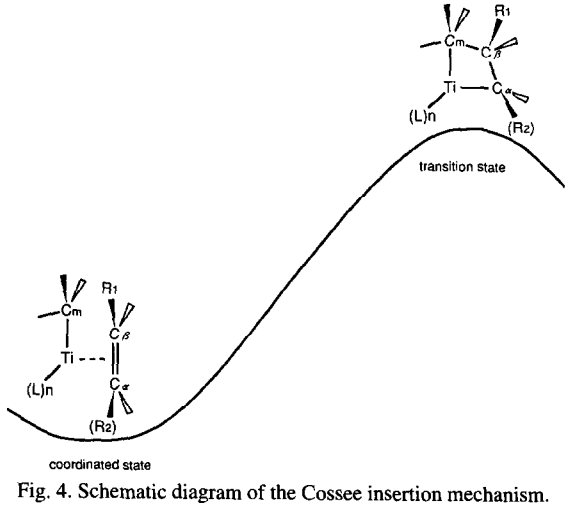

Fig. 4. Schematic diagram of the Cossee insertion mechanism.

2. we construct an interaction matrix $\mathbb{P}$ which represents the interaction between the MOs of the fragment [A] and the MOs of the fragment [B]

$$\mathbb{P}\begin{pmatrix} P_{i,k} & P_{i,n+l} \\ P_{m+j,k} & P_{m+j,n+l} \end{pmatrix} \qquad (2)$$

in which

$$P_{i,k} = 2\sum_{f=1}^{m+n} C_{i,f}d_{k,f} \qquad i=1\sim m, k=1\sim n$$

$$P_{i,n+l} = 2\sum_{f=1}^{m+n} C_{i,f}d_{n+l,f} \qquad i=1\sim m, l=1\sim N-n$$

$$P_{m+j,k} = 2\sum_{f=1}^{m+n} C_{m+j,f}d_{k,f} \qquad j=1\sim M-m, k=1\sim n$$

$$P_{m+j,n+l} = 2SUMC_{m+j,f}d_{n+l,f} \quad j=1\sim M-m, l=1\sim N-n$$

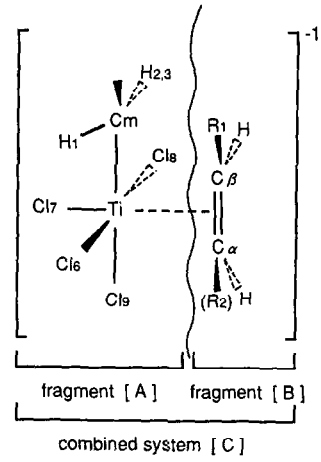

Fig. 5. The combined system [C], the fragment [A] and the fragment [B].

3. we get transformation matrices $\mathbb{U}^A$ (for A) and $\mathbb{U}^B$ (for B) by

$$\mathbb{P}^{\dagger}\mathbb{P}\mathbb{U}^A = \mathbb{U}^A\Gamma \quad (3)$$

$$U^B_{s,\nu} = (\gamma\nu)^{-1/2}\sum_r^N P_{r,s}\cdot U^A_{r,\nu} (\nu = 1, 2, ..., N) \quad (4)$$

4. and finally we obtain the PIOs by Eqs. 5 and 6

$$\phi_\nu' = \sum_r^N U^A_{r,\nu}\cdot\phi_r \text{ (for A)} \quad (5)$$

$$\varphi_\nu' = \sum_s^N U^B_{s,\nu}\cdot\varphi_s \text{ (for B)} \quad (6)$$

The $N\times M$ ($N\leq M$) orbital interactions in the complex C can thus be reduced to the interactions of N PIOs, N indicating the smaller of the numbers of MOs of the two fragments, A and B.

PIO calculations were carried out on a LUMMOX system with a NEC PC-9801RA [12].

3. Results and discussion

3.1. Ethylene insertion on the edge type active site

3.1.1. Ethylene coordinated state (a π-complex)

We have twelve PIOs. Eigenvalues of them are summarized in Table 1. The complexes (1), (3) and (7) have open-shell electronic structures, whereas the others have closed-shells. Eigenvalues show that the principal interaction between methyltitanium chloride and ethylene is expressed in PIO-1 and the subsidiary one is represented by PIO-2. In the case of the d^1-Oh π complexes, the principal interaction is electron delocalization from the occupied Ti_1 d_{xz} orbital of the methyltitanium chlorides to the π^* orbital of the ethylene molecule and the subsidiary one is electron donation from the π orbital of the ethylene molecule to the unoccupied orbitals of the methyltitanium chlorides.

A marked difference is seen between the α spin part and the β spin part of the complex (1), but the difference becomes smaller as the number of Ti atoms increases, as in (3) and (7).

In Table 2, ΔE (a measure of the strength of ethylene coordination) and the overlap population of the PIO-1 and the PIO-2 are summarized.

The value of ΔE and the overlap population are almost the same for these complexes, except for the complex (1). This can easily be understood by comparing the contour maps of the PIO-1 and the PIO-2 of the complexes (1), (2), (3) and (4), which are shown in Fig. 6 (a), (b), (c) and (d) respectively. They are very similar in shape to each other.

The Ti d_{xz} orbital of the fragment A of the complex (1) is singly-occupied. This makes ΔE of the complex (1) and the overlap population of the β spin part of PIO-1 small.

3.2. Transition state

We have examined the complexes (3), (4) and (7). Eigenvalues tell us that two types of inter-

Table 1
Eigenvalues of PIOs for the coordinated state in the model complexes

Model		PIO-1	PIO-2	PIO-3	PIO-4	PIO-5	PIO-6	.....	PIO-12
(1)	(α spin)	0.195	0.038	0.013	0.010	0.010	0.003	.....	0.000
	(β spin)	0.039	0.025	0.011	0.010	0.006	0.003	.....	0.000
(2)		0.763	0.160	0.058	0.045	0.039	0.017	.....	0.000
(3)	(α spin)	0.191	0.042	0.016	0.015	0.011	0.004	.....	0.000
	(β spin)	0.188	0.041	0.016	0.011	0.010	0.004	.....	0.000
(4)		0.761	0.166	0.062	0.058	0.042	0.018	.....	0.000
(5)		0.771	0.164	0.060	0.055	0.044	0.018	.....	0.000
(6)		0.761	0.165	0.061	0.058	0.042	0.018	.....	0.000
(7)	(α spin)	0.192	0.041	0.015	0.014	0.011	0.004	.....	0.000
	(β spin)	0.191	0.041	0.015	0.014	0.011	0.004	.....	0.000

Table 2
Total orbital energy, ΔE and overlap population of the coordinated state of the model complexes

Coordination the model state of the complexes	Total energy		Overlap population [b]				
	E_C (eV)	ΔE (eV) [a]	PIO-1		PIO-2	PIO-3	PIO-4
(1)	−970.07	−0.24	α	0.057	−0.011	−0.018	−0.022
			β	−0.011	0.0011	−0.024	−0.007
(2)	−1441.70	−0.74		0.110	−0.037	−0.027	−0.036
(3)	−2062.34	−0.73	α	0.055	−0.012	−0.017	−0.013
			β	0.054	−0.010	−0.016	−0.019
(4)	−2682.41	−0.77		0.110	−0.021	−0.035	−0.023
(5)	−2682.96	−0.70		0.110	−0.025	−0.034	−0.026
(6)	−2682.49	−0.68		0.110	−0.024	−0.034	−0.026
(7)	−3301.16	−0.74	α	0.055	−0.012	−0.017	−0.012
			β	0.055	−0.011	−0.017	−0.012

[a] $\Delta E = E_C - (E_A + E_B)$.
[b] The overlap population of the β-spin part is the same as that of the α-spin in the complexes that have an even number of electrons.

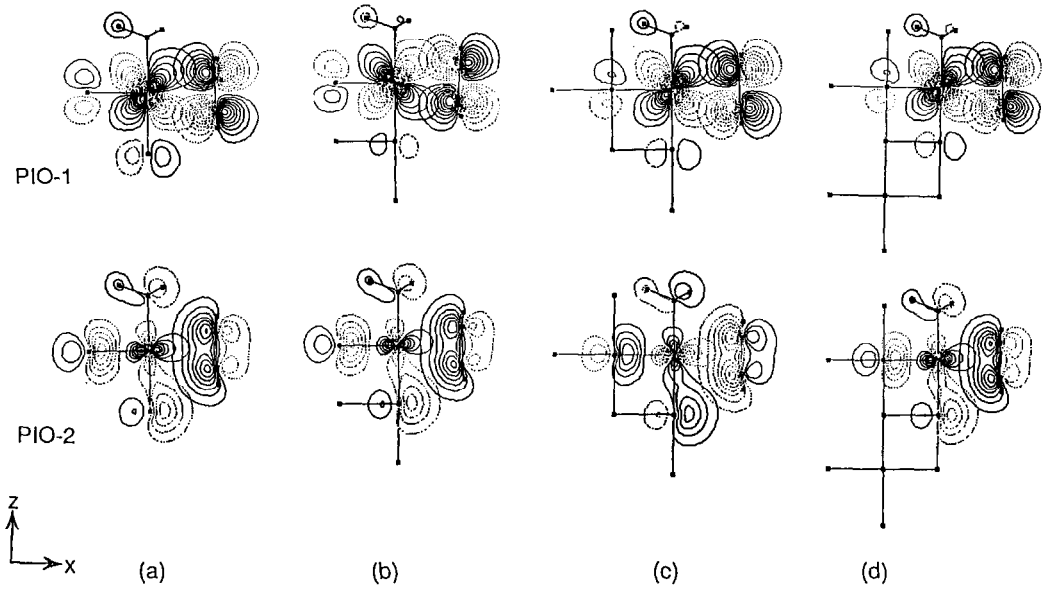

Fig. 6. Contour maps of PIO-1 and PIO-2 of models of the ethylene coordinated state. (a) model (1), (b) model (2), (c) model (3), (d): model (4).

Table 3
Eigenvalues of PIOs for the transition state of the complexes (3), (4) and (7)

Transition state of the model complexes		PIO-1	PIO-2	PIO-3	PIO-4	PIO-5	PIO-6	.....	PIO-12
(3)	α	0.189	0.070	0.023	0.020	0.017	0.008	.....	0.000
	β	0.180	0.070	0.022	0.019	0.012	0.007	.....	0.000
(4)		0.735	0.276	0.085	0.075	0.069	0.032	.....	0.000
(7)	α	0.201	0.071	0.022	0.019	0.017	0.006	.....	0.000
	β	0.179	0.068	0.021	0.019	0.017	0.008	.....	0.000

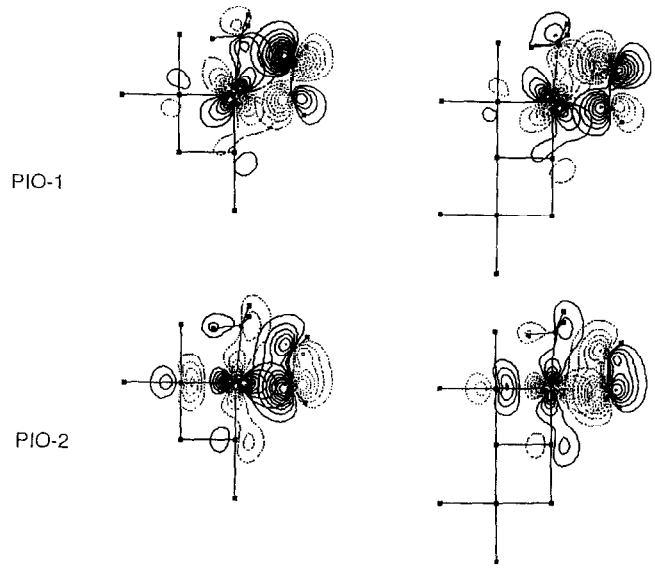

Fig. 7. Contour maps of PIO-1 and PIO-2 of models of the transition state. (a) model (3), (b) model (4).

actions, expressed by PIO-1 and PIO-2, are important at the transition state of these complexes. (See Table 3) The atomic and atomic orbital compositions of these PIOs, which are expressed compactly in contour maps (Fig. 7 (a) and (b)), demonstrate that the major interactions are electron delocalization from the occupied C p and Ti d_{xz} orbitals of the methyltitanium chloride part to the π^* orbital of the ethylene part (so called back donation) and electron donation from the π orbital of the ethylene to the unoccupied Ti d and the methyl C p orbitals of the methyltitanium chloride part.

The value of ΔE and the overlap population summarized in Table 4 show that no significant differences are found between these complexes. An activation energy in going from the π complex to the transition state are also shown to be almost the same as presented in Table 4. From these results, we can conclude that a methyltitanium chloride cluster containing more than three titanium atoms is enough to simulate the insertion on the $TiCl_3$ crystalline surface.

3.3. Ethylene insertion on the corner type active site

The corner type active site possesses two Cl vacancies. We have chosen a Ti_4 cluster, the model complex (8) as presented in Fig. 3 and

Table 4
Total orbital energy, ΔE and overlap population for the transition state of the complexes (3), (4) and (7)

Transition state of the model complex	Total energy		Overlap population [b]			ΔE^* (eV) [c]
	E_C (eV)	ΔE (eV) [a]	PIO-1		PIO-2	
(3)	−2060.10	−0.19	α	0.057	0.030	2.24
			β	0.059	0.030	
(4)	−2680.26	−0.22		0.118	0.065	2.15
(7)	−3298.96	−0.19	α	0.049	0.028	2.20
			β	0.060	0.033	

[a] $\Delta E = E_C - (E_A + E_B)$.
[b] The overlap population of the β-spin part is the same as that of the α-spin part in the complexes that have an even number of electrons.
[c] $\Delta E^* = E_C$(transition state) $- E_C$(coordinated state).

Table 5
Total energy, ΔE and activation energy of the complex (8) (θ=0°, 45°, 90°)

		θ		
		0°	45°	90°
Coordination state	Total energy E_C (eV)	−2382.13	−2381.67	−2382.15
	ΔE (eV)	−0.55	−0.05	−0.56
Transition state	Total energy E_C (eV)	−2380.31	−2380.31	−2380.36
	ΔE (eV)	−0.21	−0.08	−0.22
Activation energy	$\Delta E^{\neq}$ (eV)	1.82	1.36	1.79

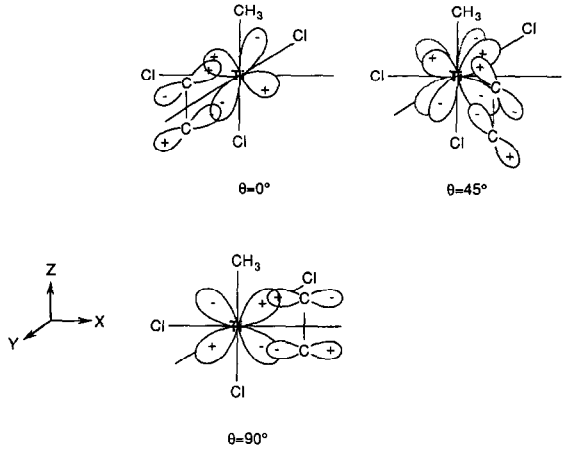

Fig. 8. Three isomers in ethylene insertion on the corner type active site.

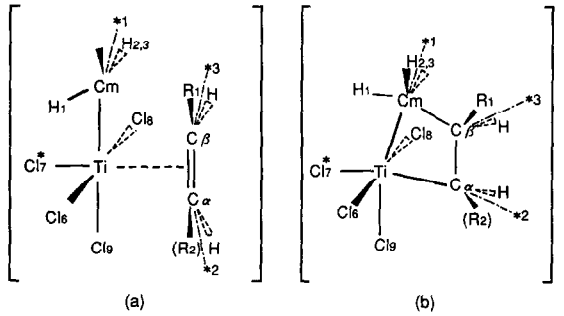

Fig. 9. Models of the olefin coordinated state (a) and the transition state (b). *syn*-form: $R_1 = CH_3$, $R_2 = H$; *anti*-form: $R_1 = H$, $R_2 = CH_3$ in propylene insertion.

examined three isomers in which an ethylene molecule has coordinated on one of the vacancies (θ=0° or 90°) or on the intermediate position (θ=45°). The total energy and ΔE of the π complex and the transition state of these three isomers and the activation energy ($\Delta E^{\neq}$) are summarized in Table 5.

The π complex with θ=45°, is shown to be less stable and have a smaller ΔE value in comparison to the other two complexes. It must be reasoned by the ineffective overlap between occupied Ti d orbitals and the π^* orbital of ethylene in the complex with θ=45°, as schematically illustrated in Fig. 8.

Since the other two complexes (θ=0° or 90°) are almost the same in energy, the activation energy ($\Delta E^{\neq}$) of the insertion is also almost the same for these two complexes. The activation energy for these complexes (θ=0° and θ=90°) is smaller than that for the complex (4), 2.15 eV (in Table 4), clearly due to a decrease in the overlap repulsion between the ligand Cl and the ethylene in the former two. Now we predict that the ethylene insertion on the corner type active site takes place in two directions orthogonal to each other and is more facile than the insertion on the edge type active site.

3.4. Regioselectivity of propylene insertion

We have chosen an edge type Ti_3 cluster and a corner type Ti_4 cluster to study the regioselectivity in propylene polymerization. The definitions *syn*-, *anti*-, *d*- and *l*- of each cluster are illustrated in Fig. 9 in the Appendix. As reported previously [7,10], an important stage of regioselection of propylene insertion is the transition state. We compared therefore the total energy of the transition state. The results are summarized in Table 6.

In the case of the edge type active site, the *syn*-type transition state is more stable than the *anti*-type transition state (ΔE_1: −0.3 eV). In the case of the corner type active site, the *anti*-type transition state (*anti-d*-0° and *anti-l*-90°) is stabilized more in the absence of a Cl anion which located orthogonal to the insertion plane and, consequently, the energy difference ΔE_1 is reduced.

Table 6
Total energy of the transition state of regioisomers in the Ti_3 edge type and the Ti_4 corner type model complexes

Model		Total energy (eV)	ΔE_1 ($E_{syn} - E_{anti}$)
Ti_3 cluster	*syn-d*	−2166.68	
	anti-d	−2166.38	−0.30
	syn-l	−2166.70	
	anti-l	−2166.41	−0.29
Ti_4 cluster	*syn-d*-0°	−2486.92	
	anti-d-0°	−2486.76	−0.16
	syn-d-90°	−2486.95	
	anti-d-90°	−2486.66	−0.29
	syn-l-0°	−2486.90	
	anti-l-0°	−2486.59	−0.31
	syn-l-90°	−2486.98	
	anti-l-90°	−2486.79	−0.19

We estimate that the insertion should be less regioselective on the corner type active site than on the edge type active site.

4. Conclusion

From the results of present calculations, we propose the presence of at least two types of active sites on the edge of the basal face of violet $TiCl_3$ crystallites: a edge type active site which possesses a dangling bonded Cl atom, four bridged Cl atoms and a Cl vacancy and a corner type active site which possesses a dangling bonded Cl atom, three bridged Cl atoms and two Cl vacancies. We have examined the size effect on these active sites by changing the number of titanium atoms of $TiCl_3$ model clusters. The most important interaction in olefin coordinated state is electron delocalization from the occupied Ti d_{xz} orbital of the methyltitanium chloride to the π^* orbital of the olefin part, while at the transition state is electron delocalization from the occupied C p and Ti d_{xz} orbital of the methyltitanium chloride to the π^* orbital of the olefin part. These orbital interactions have been shown compactly in PIO-1 at each stage.

The olefin coordination energy and the activation energy of the olefin insertion have been shown to be almost independent of the cluster size when the number of Ti atoms in a model cluster is chosen to be more than three.

The transition state is more stabilized on the corner type active site due to the absence of one of the Cl atoms which are located orthogonal to the insertion plane. It is concluded therefore that the olefin insertion is more favorable on the corner type active site than on the edge type active site. In the case of propylene insertion, *syn*-orientation of propylene is favored. The regioselectivity should be lower on the corner type active site than on the edge type active site.

Acknowledgements

We thank Prof. H. Fujimoto for helpful advice and to Sumitomo Chemical Co. Ltd. for permission of publication.

Appendix 1

Models of the olefin coordinated state and the transition state are given in Fig. 9.

Table 7
Bond lengths (Å) and bond angles (degree) of reaction models

	Coordinated state	Transition state
Bond length (Å)		
Ti–C_m	2.03	2.13
Ti–Cl	2.15	2.15
Ti–C_α	2.51	2.16
C_α–C_β	1.35	1.42
C–H(1)	1.19	1.10
C–H	1.09	1.09
C–C	1.54	1.54
Bond angle (degree)		
Cl–Ti–Cl	90	90
C_m–Ti–Cl*	90	95
C_m–Ti–C_α	90	90
Ti–C_α–C_β	74.4	90
Ti–C_m–H(1)	74.7	80
*(1)–C_m–H(1)	120	120
H–C_m–H	109.5	109.5
*(2)–C_α–C_β	173.4	150.8
*(3)–C_β–C_α	173.4	164.1
H–C_α–H	120	116.0
H–C_β–H	120	115.2
H–C–H	109.5	109.5
C–C–H	109.5	109.5

Geometrical parameters of models are given in Table 7.

References

[1] A. Anderson, H.G. Cordes, J. Herwig, W. Kaminsky, A. Merk, R. Mottweiler, J.H. Sinn and H.J. Vollmer, Angew. Chem., Int. Ed. Engl., 15 (1976) 630.

[2] (a) G. Natta, J. Polym. Sci., 34 (1959) 21; (b) T. Keii, Kinetics of Ziegler–Natta Polymerization, Kodansha, Tokyo, 1972; (c) J. Boor Jr., Ziegler–Natta Catalysts and Polymerization, Academic Press, New York, 1979; (d) G. Natta, P. Corradini and G. Allegra, J. Polym. Sci., 51 (1961) 399; (e) L.A.M. Rodriguez, H.M. van Looy and J.A. Gabant, J. Polym. Sci. A-1, 4 (1966) 1905; (f) L.A.M. Rodriguez, H.M. van Looy and J.A. Gabant, J. Polym. Sci. A-1, 4 (1966) 1917; (g) H.M. van Looy, L.A.M. Rodriguez and J.A. Gabant, J. Polym. Sci. A-1, 4 (1966) 1927; (h) L.A.M. Rodriguez and H.M. van Looy, J. Polym. Sci. A-1, 4 (1966) 1951; (i) L.A.M. Rodriguez and H.M. van Looy, J. Polym. Sci. A-1, 4 (1966) 1971; (j) Z.W. Wilchinsky, R.W. Looney and E.G.M. Tornqvist, J. Catal., 28 (1973) 351.

[3] P. Cossee, J. Catal., 3 (1964) 80.

[4] P. Novaro, E. Blaisten-Barojas, E. Clementi, G. Giunch and M.E. Ruiz-Vizcaya, J. Chem. Phys., 68 (1978) 2337.

[5] D.R. Armstrong, P.G. Perkins and J.J.P. Stewart, J. Chem. Soc., Dalton Trans., (1972) 1972.

[6] C. Daniel, N. Koga, J. Han, X.Y. Fu and K. Morokuma, J. Am. Chem. Soc., 110 (1988) 2359.

[7] H. Kawamura-Kuribayashi, N. Koga and K. Morokuma, J. Am. Chem. Soc., 114 (1992) 2359.

[8] C.A. Jolly and D.S. Marynick, J. Am. Chem. Soc., 111 (1989) 7968.

[9] (a) H. Fujimoto, N. Koga and K. Fukui, J. Am. Chem. Soc., 103, 7452 (1981); (b) H. Fujimoto, N. Koga and I. Hataue, J. Phys. Chem., 88, 3539 (1984); (c) H. Fujimoto, T. Yamasaki, H. Mizutani, and N. Koga, J. Am. Chem. Soc., 107 (1985) 6157

[10] (a) A. Shiga, H. Kawamura, T. Ebara, T. Sasaki and Y. Kikuzono, J. Organomet. Chem., 366 (1989) 95; (b) A. Shiga, H. Kawamura-Kuribayashi and T. Sasaki, J. Mol. Catal., 77 (1992) 135; (c) A. Shiga, H. Kawamura-Kuribayashi and T. Sasaki, J. Mol. Catal., 79 (1993) 95.

[11] J. Howell, A. Rossi, D. Wallace, K. Haraki and R. Hoffmann, QCPE Program No. 344.

[12] H. Katsumi, Y. Kikuzono, M. Yoshida, A. Shiga and H. Fujimoto, Chem. Info. Comp. Sci. (Jpn.) Preprint, 12 (1989) 72.